Peer-reviewed version available at *Appl. Sci.* **2020**, *10*, 3042; doi:10.3390/app10093042

Article

Effect of precious metals on NO reduction by CO in oxidative conditions

Joudia Akil[1], Stéphane Siffert[1*], Laurence Pirault-Roy[2], Damien P. Debecker[3], François Devred[3], Renaud Cousin[1], Christophe Poupin[1*]

[1] Univ. Littoral Côte d'Opale, UR 4492, UCEIV, Unité de Chimie Environnementale et Interactions sur le Vivant, 149 Avenue Maurice Schumann, 59140 Dunkerque, France

[2] Institute of Chemistry of Poitiers: materials and natural resources (IC2MP) UMR-CNRS 7285, University of Poitiers, 4, rue Michel Brunet (Bât B27) 86073 Poitiers Cedex, France

[3] Institute of Condensed Matter and Nanoscience (IMCN), Université Catholique de Louvain, Place Louis Pasteur, 1, Box L4.01.09, 1348 Louvain la-Neuve, Belgium

* Correspondence: poupin@univ-littoral.fr (C.); siffert@univ-littoral.fr (S.); Tel.: +33-328237691 (C.) ; +33-328658256 (S.)

Abstract: Carbon dioxide has become a global challenge, where the emissions have become more than what could be handled. In this regard, conversion of CO_2 to value added chemicals and thus recycling CO_2 became a viable option. One of these options is the use of a process in strong development: oxycombustion. However, the gases resulting from this process contain some traces of impurities that can hinder the recovery of CO_2 such as NO and CO. This work has therefore focused on the study of the reaction of NO reduction by CO in an oxidizing medium, using catalytic materials based on various supported noble metals. These materials were extensively characterized by a variety of methods including BET surface area measurements, hydrogen chemisorption, Transmission Electron Microscopy (TEM) and H_2 temperature programmed reduction (H_2-TPR). The obtained results show that the catalytic behaviour of M/Al_2O_3 catalysts in CO oxidation and NO reduction with CO in oxidative conditions depends mainly on the nature of the metal. The best result for these both reactions is obtained with Pt/Al_2O_3 catalyst. The Pt nanoparticles existing in the metallic form (Pt°) showed by TPR could explain the activity.

Keywords: Environmental chemistry; Oxyfuel Combustion; NO-CO reaction; Heterogeneous catalysis.

1. Introduction

Greenhouse gases (GHG) emissions generated by human activity led to an increase in the radiation which is trapped in the atmosphere and induced an increase in the greenhouse effect. This is mainly due to carbon dioxide (CO_2), the main greenhouse gas with an impact of 79%. The CO_2 emitted from anthropic activities, is perceived as a constraint in industrial activity with taxes, stringent environmental regulations, impact on global warming... To limit these CO_2 emissions, it could be considered as a gas with industrial advantage and/or as a new source of carbon for the production of minerals or organic compounds with commercial interest. Reuse of CO_2 represents a promising alternative, with important applications in chemical industry and for power generation.

The processes for the valorization of CO_2 can be divided into three different categories:[1]

- Direct use without transformation: industrial use (water treatment, supercritical CO_2 …).
- Chemical transformation: organic chemical synthesis, methanation, hydrogenation (methanol), reforming: dry (CO_2), steam reforming ($CO_2 + H_2O$)…
- Biological transformation: microalgae, biocatalysis.

However, CO_2 valorization process requires a gas as pure as possible [1].

Oxyfuel-combustion is therefore a promising method to get a nearly pure CO_2 that enables to obtain a CO_2 rich stream (80%) [2]. In the oxyfuel system, the combustion flow consists of O_2 separated from air. Therefore, the flue gas is dominated by CO_2. The oxidation of N_2 for NOx emissions is limited which are considered as one of the main pollutants of the atmosphere, since they are responsible for a lot of environmental problems like photochemical smog, acid rain, ozone layer depletion [3]. This Process emits also water vapor, unburned components (in function of the waste burned) such as carbon monoxide (generated by incomplete combustion) and nitrogen monoxide [2]. CO is the cheapest and the most available from industrial sources and it could be used as a reductant of NO, but it is known to be one of the worst reductant. P. Malfoy classified, on noble metals, several reducers on the base of the NO half-conversion temperatures. The sequence obtained is as follows: $H_2 > NH_3 > CO > C_3H_5$ [4]. So it seems possible to purify the CO_2 issued from oxyfuel-combustion by NO-CO reaction.

In oxyfuel combustion systems, NO, CO, O_2 are simultaneously present and the following reactions may occur [5]:

$2\ NO + 2\ CO \rightarrow N_2 + 2\ CO_2$

$2\ CO + O_2 \rightarrow 2\ CO_2$

Therefore as oxygen is present in excess, it competes with NO for oxidizing the reducing agent (CO) [6]. Due to this effect, many authors studied the competitions between CO-NO and CO-O2 reactions. Shelef et al. found that the second reaction is predominant over a number of transition metal oxides and supported Pt [7]. Other authors proved that the NO addition to $CO+O_2$ reduces drastically the rate of CO_2 formation on Rh catalyst [8] and Pt supported catalyst [9].

The NO–CO reaction has been widely applied and investigated over various catalysts. The reduction of NO by CO occurring over three-way catalysts (TWC), composed of noble metals (Rh, Pd and Pt), is very important because it converts CO, NO, and hydrocarbon simultaneously [10]. Rh is employed for NO removal because it combines a good activity and selectivity to form nitrogen [11]. On the other hand, Pt and Pd ensure the oxidation of CO and hydrocarbon [12]. Kobylinski and Taylor [15] studied NO reduction over supported Pt, Rh, Pd and Ru. They found that, when CO is used as reducing agent, the reaction over Ru catalyst is accelerated. The activity sequence of the catalysts was: Ru > Rh > Pt > Pd. Ir was also studied over this reaction in presence of O_2 [6,16]. It has demonstrated that Ir effectively promotes the NO-CO reaction in the presence of an excess of oxygen.

To summarize, the objective is to reduce NO by CO in an oxidizing environment with a CO_2 rich stream without any additives like SCR reaction. The important amount of CO_2 could be a problem for some basic materials that's why we chose alumina because of its strong Lewis acid center which ensures the stabilization of species in active state and disperses them adequately, as well as its intrinsic catalytic activity in various reactions [12,17]. This paper will present you this work with materials prepared with different precious metal (Pt, Pd, Rh, Ru and Ir) loadings supported on alumina.

1. Introduction

The introduction should briefly place the study in a broad context and highlight why it is important. It should define the purpose of the work and its significance. The current state of the research field should be reviewed carefully and key publications cited. Please highlight controversial and diverging hypotheses when necessary. Finally, briefly mention the main aim of the work and highlight the principal conclusions. As far as possible, please keep the introduction comprehensible to scientists outside your particular field of research. References should be

numbered in order of appearance and indicated by a numeral or numerals in square brackets, e.g., [1] or [2,3], or [4–6]. See the end of the document for further details on references.

2. Materials and Methods

1.1. Catalysts preparation

Alumina (Aluminum Oxide C from Degussa) with a specific surface area of 100 $m^2.g^{-1}$ was used as support. After calcination of support for 4 h at 500 °C under air, the catalysts were prepared by wet impregnation of alumina with corresponding precursors in the following table (table1). For all catalysts, the nominal contents were of 1.0 wt%.

Table 1. Metal precursors

Metal	Iridium	Palladium	Platinum	Rhodium	Ruthenium
precursor used	$Ir(acac)_3$	$Pd(acac)_2$	$Pt(NO_2)_2(NO_3)_2$	$Rh(NO_3)_3$	$Ru(acac)_3$

The impregnated support was left overnight in an oven at 120 °C. It was then calcined in dry air at 500 °C for 4 h and reduced in H_2 flow for 4 h at 500 °C.

1.2. Characterization of the catalysts

Before any impregnation, the support used (Al_2O_3) was characterized by nitrogen physisorption (BET, BJH) H_2 chemisorption.

Specific surface areas of samples were measured by nitrogen adsorption and desorption at −196 °C with BET surface analyzer (Micromeritics Model TRISTAR 3000) using BET-BJH method. Before the analysis, the samples were outgassed at 250 °C under vacuum overnight.

The hydrogen chemisorption capacity was determined by a static volumetric vacuum technique at room temperature. Firstly, the catalyst was cleaned under ultra-high vacuum overnight to eliminate the adsorbed molecules. Then, the catalyst was reduced under 750 mbar of H_2 for 1 h at 300 °C, and purged under vacuum until reaching a low pressure ($P < 10^{-5}$mbar). Two series of hydrogen adsorption isotherms were performed with an increasing hydrogen pressure, from 10 to 70 mbar with an augmentation of 10 mbar. Between the two series, the sample was submitted to ultrahigh vacuum in order to remove weakly bound hydrogen. The adsorbed hydrogen quantity was calculated by extrapolating the isotherm to P = 0. The first isotherm allows determining the total amount of adsorbed hydrogen and the second one the amount of physisorbed hydrogen. The chemisorbed hydrogen amount was calculated by difference between these two values. The metal particle size was calculated considering a stoichiometry of H/M = 1, and assuming that particles correspond to cubes deposited on the sup-port and exposing 5 faces [18], with an equal distribution between (1 1 1), (1 1 0) and (1 0 0) planes.

In order to provide a check of the results obtained with hydrogen chemisorption, transmission electron microscopy (TEM) analysis were performed with a JEOL 2100 electron microscope operating at 200 kV with a theoretical resolution of 0.19 nm. Catalysts were finely ground, dispersed in ethanol using an ultrasonic bath and finally deposited on the carbon film of a copper grid. The particle size distribution was estimated on the basis of several pictures. The average particle size was then calculated using the relation $\Sigma nidi3/\Sigma nidi2$ where ni is the number of particles with size di. The correlation between the metallic accessibility determined by hydrogen adsorption and the average particle size from TEM was evaluated on the basis of a model of cubic particles lying on one face. The particle size distribution was obtained from TEM pictures calculating the average particle diameter from the measurement performed on at minimum 100 particles.

H_2 temperature programmed reductions (TPR) were performed on a Hiden Catlab equipped with QGA Hiden quadrupole mass spectrometer. The catalysts were first pretreated at 200°C for 1 hour under argon (20 mL/min Air Liquide 5.0). The sample was then cooled down to 80°C and exposed to a mixture of 0.25 % H_2 in inert atmosphere. The TPR was then carried out using a ramp of

Preprints (www.preprints.org) | NOT PEER-REVIEWED | Posted: 27 February 2020 doi:10.20944/preprints202002.0406.v1

Peer-reviewed version available at Appl. Sci. 2020, 10, 3042; doi:10.3390/app10093042

10 °C.min^{-1} up to 500 °C. Hydrogen Sensitivity factor was determined before the ramp for further quantification.

1.3. *Catalytic tests*

Before each test, the catalyst was treated in situ under He flow (40 mL.min^{-1}) at 200 °C for 1.5 h. Then, CO_2 purification was carried out at atmospheric pressure in a fixed-bed flow reactor containing 150 mg of catalyst. The catalysts were sieved in order to retain grains with diameters between 0.315 and 0.500 mm and diluted to a constant volume by SiC (exhibited no activity in CO_2 purification from 50 to 500 °C) so that all the experiments were carried out under the same conditions (GHSV = 2.24 10^4 h^{-1}).

The flow of the reactant gases is composed of: 20 % CO_2, 10 % O_2, 0.5 % CO and 0.02 % NO (He as eluent gas) with a total flow of 200 mL.min^{-1}, in the temperature range 50–500 °C. The reaction products (CO_2 and N_2) were analyzed on line by a gas chromatograph (GAS analyzer XXL1300), NO was analyzed with Xentra 4900C analyzer (Servomex). The measurement of NO_2 is done indirectly using a NO_2 to NO converter BÜNOx (Bühler Technologies) by comparison.

The conversion, selectivity and yields of the main products are defined in the following way:

- Conversion: $X_i\ (\%) = \frac{n_i^{int} - n_i^{out}}{n_i^{int}} * 100$ where n_i^{int} and n_i^{out} are number of mole of the corresponding compounds "i" at the inlet and the outlet of the reactor.
- Selectivity: $S_i\ (\%) = \frac{n_i}{\sum_i n_i} * 100$
- Yield: $Y_i(\%) = X_i * S_i * 100$

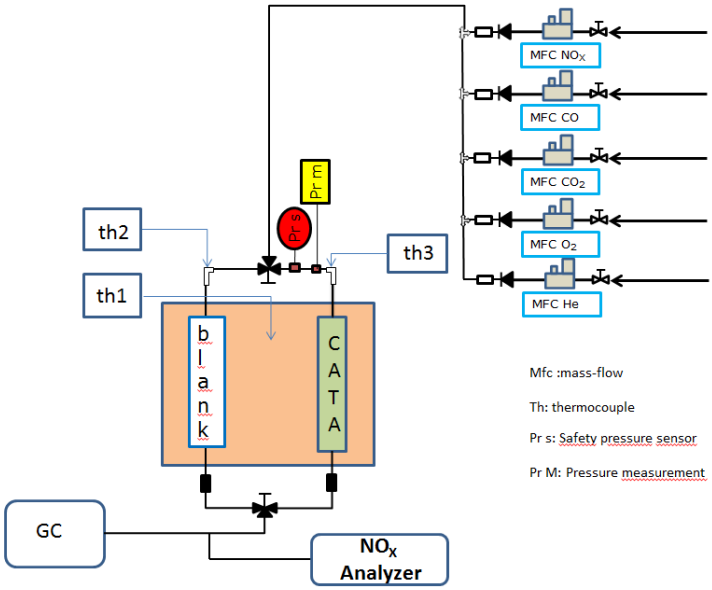

Figure 1: Experimental setup for catalytic purification of CO_2 from oxyfuel combustion

In order to compare the different materials, T_{50} and T_{90} factors will be taken into account. These factors correspond respectively to the temperature at which 50% or 90% of carbon monoxide is converted. For NO reduction, the catalysts will be compared according to their maximum efficiency (yield) at total conversion of CO.

3. Results

The Alumina supported catalysts prepared by wet impregnation with precious metal were studied in the catalytic purification of CO_2. In this study we bring out the effect of nature of metal in this reaction.

Preprints (www.preprints.org) | NOT PEER-REVIEWED | Posted: 27 February 2020 doi:10.20944/preprints202002.0406.v1

Peer-reviewed version available at Appl. Sci. 2020, 10, 3042; doi:10.3390/app10093042

3.1. BET surface area

The specific surface area of the alumina and its pore volume were determined by adsorption of nitrogen. Table 2 summarizes the results obtained by the BET and BJH methods.

Table 2. Specific surface area and porous volume of alumina

Sample	S_{BET} ($m^2.g^{-1}$)	V_{porous} ($cm^3.g^{-1}$)	Average pore size (nm)
Alumina	100	0,74	31

From these results, the alumina used as support for our catalysts is a mesoporous solid with a large specific surface area.

3.2. TEM and H_2 chemisorption

In order to compare the catalytic activity for our catalysts, we tried to synthesize size-controlled uniform material. We can see in Figure 2 that the synthesized catalytic materials have a homogeneous distribution of particle size.

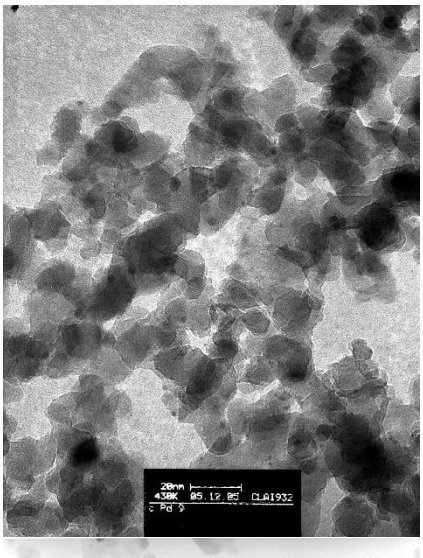

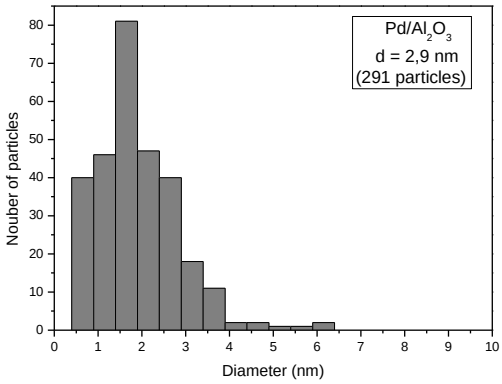

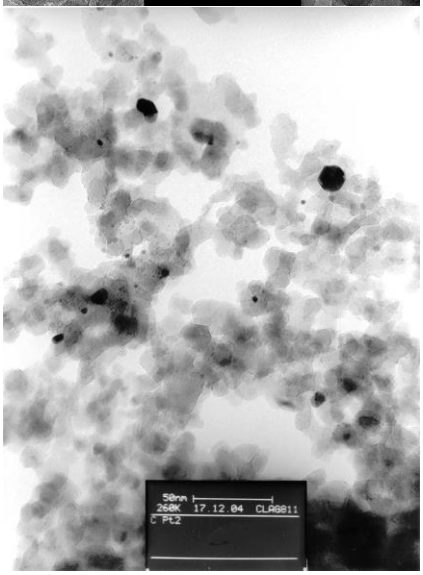

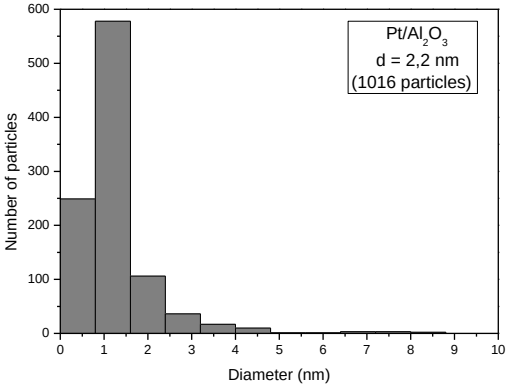

Preprints (www.preprints.org) | NOT PEER-REVIEWED | Posted: 27 February 2020 doi:10.20944/preprints202002.0406.v1

Peer-reviewed version available at Appl. Sci. 2020, 10, 3042; doi:10.3390/app10093042

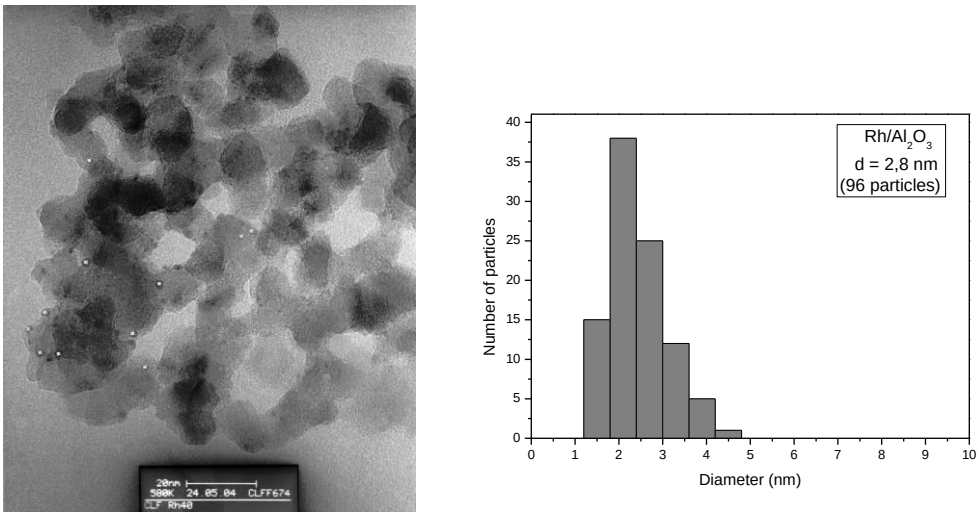

Figure 2. TEM pictures and size distribution of the Al_2O_3 supported noble metallic Pd, Pt and Rh.

Table 3. Properties of catalysts: particles size and metallic accessibility.

Catalysts	Reference	Metallic accessibility (%)	< d > [a] (nm)	< d > [b] (nm)
1% Ir/Al_2O_3	Ir	42	2.2	---
1% Pd/Al_2O_3	Pd	40	2.4	2.9
1% Pt/Al_2O_3	Pt	40	2.3	2.2
1% Rh/Al_2O_3	Rh	41	2.2	2.8
1% Ru/Al_2O_3	Ru	28	3.8	3.8

a Obtained by H_2 chemisorption analysis. b Estimated by TEM pictures.

The results obtained by H_2 chemisorption in the table 2 shown that, the Ir, Pd, Pt and Rh on Al_2O_3 catalysts presents the similar particle size leading to d=2.2 nm. In the case of Ru/Al_2O_3, the particles were larger than those on the other catalyst samples.

In order to have more specific information about the morphology and composition of the prepared samples, TEM measurements were performed. As shown in the table 2, for all of the catalysts, the particles size obtained by TEM was in accordance with the results obtained by H_2 chemisorption.

3.3. Temperature programmed reduction by H_2

The H_2-TPR measurements were performed to determine the reduction behaviors and chemical compositions of various catalysts as depicted in Fig 3. Since the Al_2O_3 support is irreducible from room temperature to 500°C, the peaks of reduction in this temperature range should correspond to the reduction of the different kinds of active phase species.

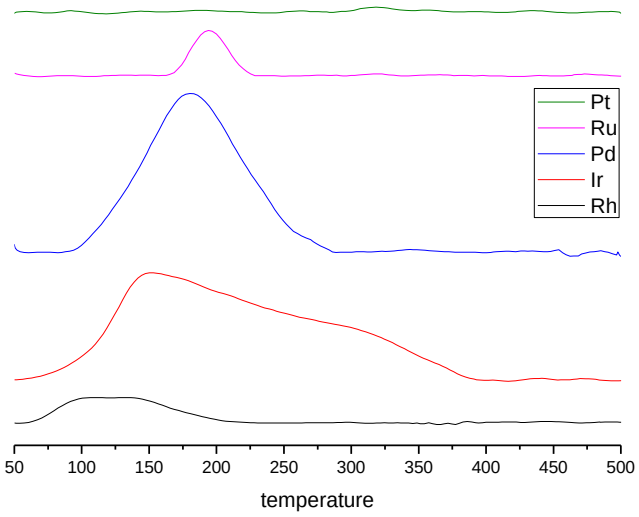

Figure 3. H_2-TPR patterns of the different catalysts (°C)

The TPR profile of Pd supported is characterized by one broad pic centered at around 180°C. According to Ferrer and al. [19] this peak is attributed to the reduction of PdOx species that strongly interacts with the support. However, no negative peak was observed at 80°C corresponding to the desorption of hydrogen from PdHx which could be formed at low temperature [17,20].

No reduction peak was observed for Pt. Pt nanoparticles should mainly exist in the metallic form (Pt°) not accessible for further reduction. [21] But, generally a reduction peak is found by TPR. These Pt° nanoparticles should then be especially active for CO oxidation.

The profile of Ru shows a peak with a maximum at about 194°C, which is attributed to Ru oxide reduction already demonstrated by Koopman & al [22].

The Ir catalyst exhibits a broad reduction peak between 100-400°C, which can be attributed to the reduction of IrO_2 phase [21,23]. But, usually the reduction IrO_2 phase is found at higher temperature. This phase should then be more active for CO oxidation than expected.

The Rh profile is composed of a broad reduction peak from ambient to 250°C which is attributed to the reduction of surface RhOx species, according to the literature [24–25].

3.4. Catalytic reaction

The general catalytic performance of different materials have been studied and determined for the catalytic total CO oxidation and NO reduction with CO in oxidant atmosphere (10% O_2) and CO_2 rich stream under identical conditions.

Light-off curve of support (Al_2O_3) have been determined and is reported in fig 4.

Preprints (www.preprints.org) | NOT PEER-REVIEWED | Posted: 27 February 2020 doi:10.20944/preprints202002.0406.v1

Peer-reviewed version available at Appl. Sci. 2020, 10, 3042; doi:10.3390/app10093042

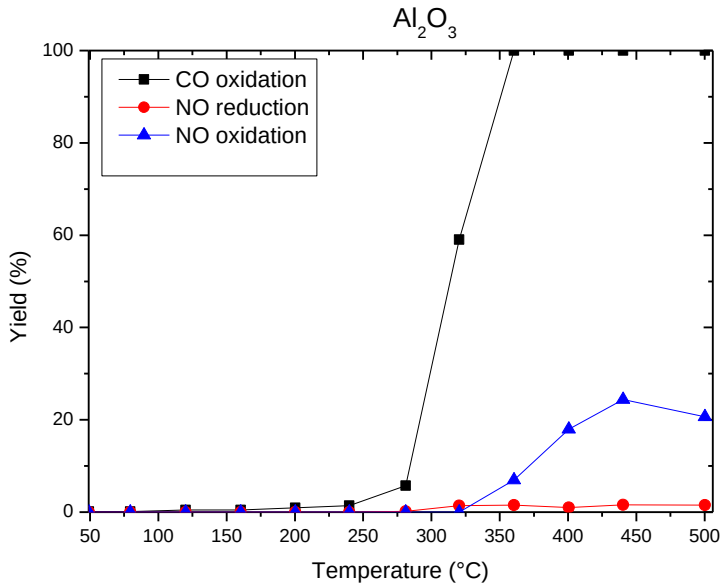

Figure 4. Light-off curves for Al_2O_3 support

It can thus be seen in fig 4 that on the alumina, it is possible to have a complete oxidation of the CO. For the conversion of NO, there is a slight oxidation of NO at very high temperature but no reduction.

Fig 5 shows the activities of the catalysts for CO oxidation. They exhibit the activity for this reaction at the temperatures higher than 100°C and the conversion increases with the reaction temperature. For all tests, catalytic performances were compared by considering T_{50} and T_{90} for CO oxidation, which respectively correspond to the temperatures at which 50 and 90% of CO were converted. The obtained results are illustrated in fig 5. The conversion of CO to CO_2 was 100% for all used catalysts. Ir and Rh have a similar activity values with T_{50} at 236 °C. The general order of catalytic activity, based on the temperature required for 50% conversion (T_{50}) is the following: Pt > Pd > Ir~Rh > Ru.

Considering T_{90}, Pt shows the better performance (176°C), Rh and Ru present a similar activity values with 280°C. The ranking for catalysts does not much change to that at T_{50}: Pt > Pd > Ir > Rh~Ru.

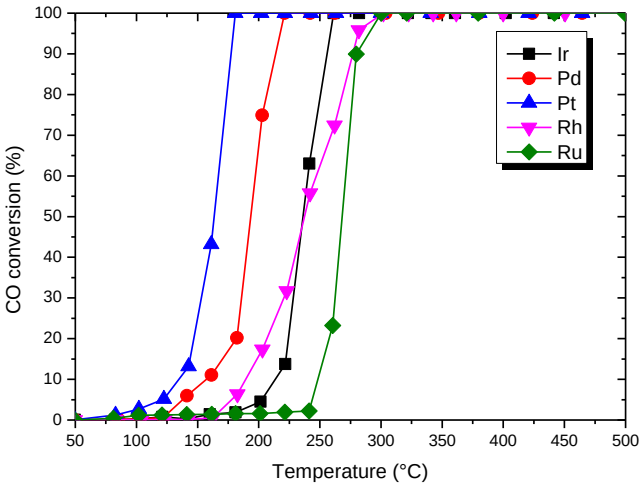

Figure 5. Light-off curves of CO conversion for the different materials. Feedstream composition: 0.02%NO, 0.5% CO, 10% O_2 and 20% CO_2, and balance He. Space velocity: 2.24 10^4 h^{-1}

Table 4. T_{50} and T_{90} of catalysts catalytic CO oxidation

Catalysts	T_{50} (°C)	T_{100} (°C)
Ir	236	260
Pd	194	212
Pt	164	176
Rh	236	280
Ru	268	280

The oxidation of CO, reduction of NO and oxidation of NO over the impregnated Al_2O_3 with Ir, Pd, Pt, Rh, Ru were evaluated, and the obtained results have been reported in Fig 6.

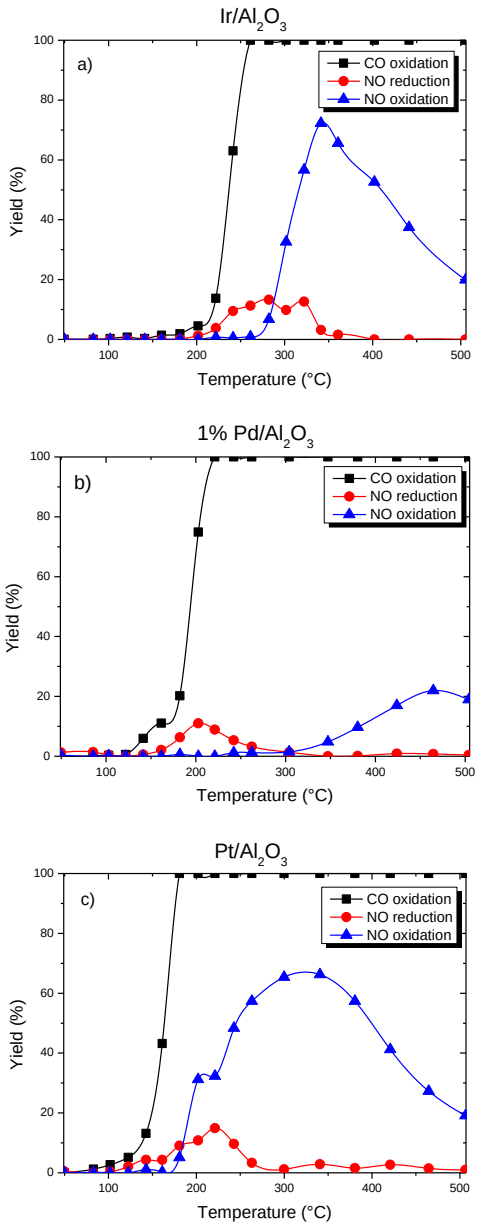

Preprints (www.preprints.org) | NOT PEER-REVIEWED | Posted: 27 February 2020 doi:10.20944/preprints202002.0406.v1

Peer-reviewed version available at Appl. Sci. 2020, 10, 3042; doi:10.3390/app10093042

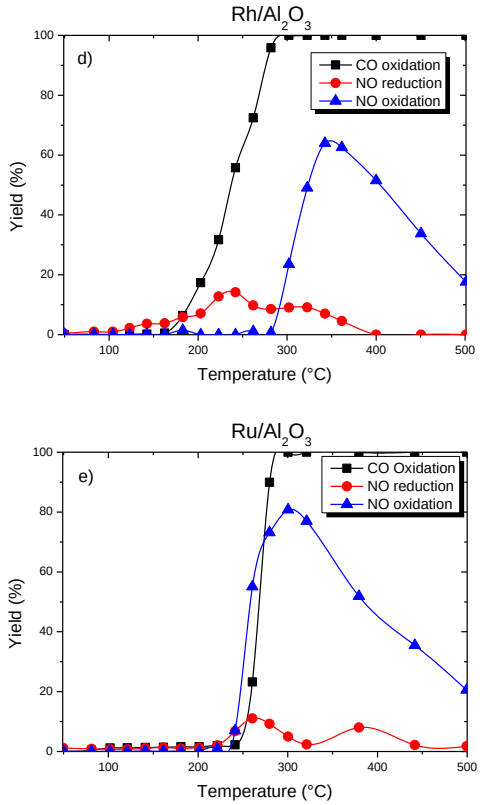

Figure 6. Catalytic activity for the impregnated alumina with Pt, Rh, Ru, Pd, Ir. Feedstream composition: 0.02% NO, 0.5% CO, 10% O_2 and 20% CO_2, and balance He. Space velocity: 2.24 10^4 h^{-1}

Fig 6-a. represents the activity of Ir in these reactions. The CO is completely oxidized at 260°C with a 13% of NO reduction. The oxidation of NO reaches 72.3% at 340°C.

Fig 6-b. shows the activity of Pd in CO and NO reactions. The oxidation of CO is carried out at 220°C. NO reduction reaches a maximum with 11% at 200°C but the CO is not completely oxidized at 220°C, only 9% of NO is reduced.

Fig 6-c. shows the activity of Pt in NO-CO reaction. The CO is totally oxidized at 180°C. The NO reduction begins from the start of the CO oxidation. Pt/Al_2O_3 reduces the NO from 140°C to 300°C with a maximum reduction (14.9%) at 220°C, the oxidation phase is also bell-shaped with an optimum (66.2%) at 340°C.

Fig 6-d. represents the activity of Rh in CO and NO reactions. The oxidation of CO with the supported Rh occurs later than with Pt or Pd, in fact the total conversion of CO is obtained at 300°C. This is in full agreement with the literature on three-way catalysts that use Rh to convert NOx [10]. With regard to the conversion of NO, the reduction of NO is 14.4% at 240°C. On the other hand, at higher temperatures, NO oxidizes 64.2% for alumina at 340°C.

Fig 6-e. represents the activity of Ru in oxidation of CO and reduction of NO. Like Rh the total conversion of CO is obtained at 300°C and the NO is converted at 85% but with 80% is oxidized and only 5% is reduced.

In order to compare and highlight the influence of nature of the metal on the NO reduction with CO in an oxidative conditions, we presents you, in fig 7 the maxima of NO reduction at total oxidation of CO over all catalysts. The Pt/Al_2O_3 and Ir/Al_2O_3 catalysts are the best ones of NO reduction by CO in presence of an excess of oxygen and a CO_2 rich stream. Pd, Rh and Ru show similar activity and yield but at different temperatures: 220°C for Pd, 320 °C for Rh and 380°C for Ru.

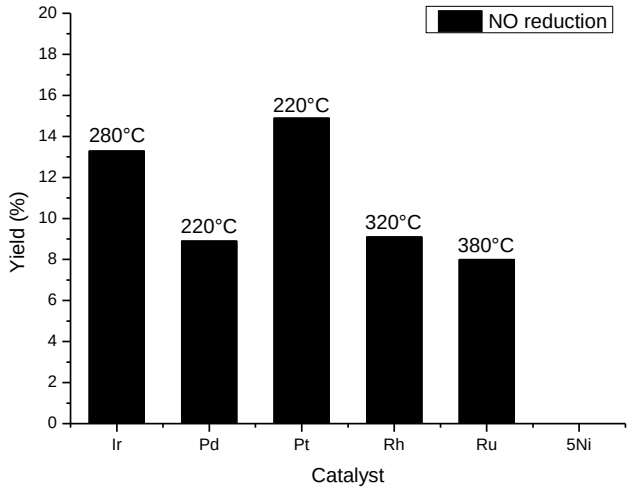

Figure 7. NO reduction at total oxidation of CO. Feedstream composition: 0.02%NO, 0.5% CO, 10% O_2 and 20% CO_2, and balance He. Space velocity: 2.24 10^4 h^{-1}

In our results the low activity of the Pd compare to Ir catalyst could be explain by an oxygen poisoning of the Pd. Almusaiteer and Chuang [27] proved that the presence of O_2 in NO-CO reaction flows plays a role of poison on Pd/Al_2O_3 catalyst. The adsorbed oxygen inhibits N-O dissociation thus causing an accumulation of Pd-N=O and diminution of conversion of NO. Ir, on the other hand, has a superior ability than other precious metal to convert NO under oxidizing environment due to its ability to adsorb NO dissociatively in the presence of an excess of O_2 [16]. Tauster and Murell [6] confirmed this result and they proved that Ir is the only catalyst favoring the NO-CO reaction over $CO-O_2$.

4. Conclusion

This work deals with the identification of the best metal catalysts for CO_2 purification in oxidative conditions. In this work, we focus on the NO reduction on alumina supported precious metal using carbon monoxide as reduction agent in oxidizing conditions. First of all, it is possible to achieve a reduction of the NO in an oxidizing medium using a catalytic material by using one of the worst reducer, often present in the industrial process outputs, thus not requiring to add one thus to add an injection system of a reducer such as ammonia.

Author Contributions: J.A. prepared the materials, conducted the experiments and wrote the first draft of the paper. C.P. and S.S. supervised the work. D.D. and F.D. realized the TPR measurements. All authors contributed to the data interpretation, the discussion and the revision of the paper.

Funding: This research was funded by: Innocold, Dunkerque LNG, Greater Dunkirk Council and ULCO.

Conflicts of Interest: The authors declare no conflict of interest.

References

1. Dumergues, L.; Favier, B.; Claver, R.A.; *CO_2 Reuse. STate of the Art and Expert Opinion Case of waste treatment activities*, **2014**.
2. Iloeje, C.; Field, R.; Ghoniem, A.F.; Modeling and parametric analysis of nitrogen and sulfur oxide removal from oxy-combustion flue gas using a single column absorber, *Fuel.* **2015**, 160, 178–188. doi:10.1016/j.fuel.2015.07.057.
3. Skalska, K.; Miller, J.S.; Ledakowicz, S.; Trends in NOx abatement : *A review*, **2010**, 408, 3976–3989. doi:10.1016/j.scitotenv.2010.06.001.
4. Malfoy, P. ; Reduction Catalytique de NO et N_2O par H_2 , CO ou C_3H_8, **1997**.

5. Hegedus, L.L.; Hertz, R.K.; Oh, S.H.; Aris, R.J.; Effect of Catalyst Reactions Loading on the Simultaneous of NO, CO, and O_2, *J. Catal.* **1979**, 57, 513–515.
6. Tauster, L.M.S.J.; The NO-CO Reaction In the Presence of Excess O_2 as Catalyzed by Iridium, *J. Catal.* **1976**, 41, 192–195.
7. Shelef, M.; Otto, K.; Ghandy, H.; The oxidation of CO by O_2 and by NO on supported chromium oxide and other metal oxide catalysts, *J. Catal.* **1968**, 375, 361–375.
8. Oh, S.H.; Carpenter, J.E.; Role of NO in inhibiting CO oxidation over alumina-supported rhodium, *J. Catal.* **1986**, 101, 114–122. doi:10.1016/0021-9517(86)90234-4.
9. Voltz, S.E.; Morgan, C.R.; Liederman, D.; Jacob, S.M.; Kinetic study of carbon monoxide and propylene oxidation on platinum catalysts, Ind. & *Eng. Chem. Prod. Res. Dev.* **1973**, 12, 294-301
10. Granger, P.; Parvulescu, V.I.; Catalytic NOx abatement systems for mobile sources: From three-way to lean burn after-treatment technologies, *Chem. Rev.* **2011**, 111, 3155–3207. doi:10.1021/cr100168g.
11. Barbier, J.; Duprez, D.; Steam Effects in 3-Way Catalysis, *Appl. Catal. B* **1994**, 4, 105–140.
12. Vedyagin, A.A.; Volodin, A.M.; Stoyanovskii, V.O.; Kenzhin, R.M.; Slavinskaya, E.M.; Mishakov, I.V., Stabilization of active sites in alloyed Pd-Rh catalysts on gamma-Al_2O_3 support, *Catal. Today* **2014**, 238, 80–86. doi:10.1016/j.cattod.2014.02.056.
13. Romero-Galarza, A.; Dahlberg, K.A.; Chen, X.; Schwank, J.W.; Crystalline structure refinements and properties of Ni/TiO_2 and Ni/TiO_2-Ce catalysts and application to catalytic reaction of "CO+NO," *Appl. Catal. A* **2014**, 478, 21–29. doi:10.1016/j.apcata.2014.03.029.
14. Wang, Y.; Zhu, A.; Zhang, Y.; Au, C.T.; Yang, X.; Shi, C.; Catalytic reduction of NO by CO over NiO/CeO_2 catalyst in stoichiometric NO/CO and NO/CO/O_2 reaction, *Appl. Catal. B* **2008**, 81, 141–149. doi:10.1016/j.apcatb.2007.12.005.
15. Kobylinski, T.P.; Taylor, B.W.; The catalytic chemistry of nitric oxide, *J. Catal.* **1974**, 33, 376–384. doi:10.1016/0021-9517(74)90284-X.
16. Taylor, K.; Schlatter, J.C.; Selective reduction of nitric oxide over noble metals, *J. Catal.* **1980**, 63, 53–71. doi:10.1016/0021-9517(80)90059-7.
17. Wang, C.-B.; Lee, H.-G.; Yeh, T.-F.; Hsu, S.-N.; Chu, K.-S.; Thermal characterization of titania-modified alumina-supported palladium and catalytic properties for methane combustion, *Thermochim. Acta.* **2003**, 401, 209–216. doi:10.1016/S0040-6031(02)00567-1.
18. Bond, G.C.; The Origins of Particle Size Effects in Heterogenous Catalysis, *Surf. Sci.* **1985**, 156, 966–981.
19. Ferrer, V.; Finol, D.; Solano, R.; Moronta, A.; Ramos, M.; Reduction of NO by CO using Pd-CeTb and Pd-CeZr catalysts supported on SiO_2 and La_2O_3-Al_2O_3; *J. Environ. Sci. (China)* **2015**, 27, 87–96. doi:10.1016/j.jes.2014.05.046.
20. Hosseini, M. ; Etude de catalyseurs Pd / Au déposés sur oxydes poreux, TiO_2 et Composés Organiques Volatils (COV), **2008**.
21. Goula, M. A.; Charisiou, N. D.; Papageridis, K. N.; Delimitis, A.; Papista, E.; Pachatouridou, E.; Iliopoulou, E.F.; Marnellos, G.; Konsolakis, M.; Yentekakis I.V.; A comparative study of the H_2-assisted selective catalytic reduction of nitric oxide by propene over noble metal (Pt, Pd, Ir)/γ-Al_2O_3 catalysts; *J. Env. Chem. Eng.* **2016**, 4, Issue 2, 1629-1641; doi.org/10.1016/j.jece.2016.02.025
22. Koopman, P.G.J.; Kieboom, A.P.G.; Van Bekkum, H.; Characterization of ruthenium catalysts as studied by temperature programmed reduction, *J. Catal.* **1981**, 69, 172–179. doi:10.1016/0021-9517(81)90139-1.
23. Vicerich, M.A.; Benitez, V. M.; Especel, C.; Epron, F.; Pieck C.L.; Influence of iridium content on the behavior of Pt-Ir/Al_2O_3 and Pt-Ir/TiO_2 catalysts for selective ring opening of naphthenes, *Appl. Catal. A* **2013**, 453, 167–174; doi.org/10.1016/j.apcata.2012.12.015
24. Zhao, B.; Ran, R.; Cao, Y.; Wu, X.; Weng, D.; Fan, J.; Insight into the effects of different ageing protocols on Rh/Al_2O_3 catalyst, *Appl. Surf. Sci.* **2014**, 308, 230–236. doi:10.1016/j.apsusc.2014.04.140.
25. McCabe, R.W.; Usmen, R.K.; Ober, K.; Gandhi, H.S.; The effect of alumina phase-structure on the dispersion of Rhodium/Alumina catalysts, *J. Catal.* **1995**, 151, 385–393; doi:10.1006/jcat.1995.1041.
26. Gao, Y.; Meng, F.; Cheng, Y.; Li, Z.; Influence of fuel additives in the urea-nitrates solution combustion synthesis of Ni-Al_2O_3 catalyst for slurry phase CO methanation, *Appl. Catal. A* **2017**, 534, 12–21 doi:10.1016/j.apcata.2017.01.016.
27. Almusaiteer, K.; Chuang, S.S.C.; Isolation of Active Adsorbates for the NO–CO Reaction on Pd/Al_2O_3 by Selective Enhancement and Selective Poisoning, *J. Catal.* **1998**, 170, 161–170.